JOURNAL OF Applied Polymer SCIENCE

Chitosan/silk fibroin composite scaffolds for wound dressing

Shanyi Guang,[1,4] Yang An,[2] Fuyou Ke,[2] Dongmei Zhao,[3] Yuhua Shen,[1] Hongyao Xu[2]

[1]School of Chemistry and Chemical Engineering, Anhui University, Hefei 230601, People's Republic of China

[2]College of Material Science and Engineering & State Key Laboratory for Modification of Chemical Fibers and Polymer Materials, Donghua University, Shanghai 201620, People's Republic of China

[3]The Second Affiliated Hospital of Shandong University, Jinan, Shandong, People's Republic of China

[4]College of Chemistry, Chemical Engineering and Biotechnology, Donghua University, Shanghai 201620, People's Republic of China

Correspondence to: H. Xu (E-mail: hongyaoxu@163.com)

ABSTRACT: Three-dimensional (3D) chitosan/silk fibroin (CS/SF) porous composite scaffolds have been prepared by simply coating a thin layer of CS onto spunlaced SF scaffolds via hydrogen-bonding assembly technique, and they were characterized by Fourier transform infrared (FTIR) spectroscopy, scanning electron microscopy (SEM), X-ray diffraction (XRD), and mechanical property measurements. The results show that porous scaffolds have a pore diameter around 50–200 μm, and improved mechanical property compared with SF, resulting from strong intermolecular hydrogen bonding interactions between CS and SF, together with the maintained β-sheet structure of SF. The medical and biological properties of the composite scaffolds were further evaluated. The results demonstrate that they possess good biocompatibility and a broad spectrum of antimicrobial properties. The *in vivo* animal experiments show that the composite scaffolds promote skin regeneration of rats without any teratogenic effect and inflection, thus they are very promising in the application of wound dressings. © 2015 Wiley Periodicals, Inc. J. Appl. Polym. Sci. **2015**, *132*, 42503.

KEYWORDS: biomaterials; biomedical applications; composites

Received 24 November 2014; accepted 14 May 2015
DOI: 10.1002/app.42503

INTRODUCTION

Epidermal damage as a result of ulcer, burn, operative, or other traumatic incidents is common in our daily life, thus wound dressing is usually used for wound healing in a short time. An ideal wound dressing should have good biocompatibility, good water retention to maintain hemostasis, and suitable moist environment, 3D porous structures to allow water and air permeation and promote epithelization by releasing biological agents to the wounds.[1,2] Silk fibroin (SF) derived from silkworm cocoon has diverse excellent properties, including good biocompatibility and biodegradability, remarkable humidness and air permeability and well mechanical properties, as well as abundant source. Furthermore, SF could promote the attachment and proliferation of human skin fibroblasts and keratinocytes.[3] These merits make SF excellent suitability as wound dressing materials. SF scaffolds have been prepared in various methods, e.g., freeze-drying,[4] salt leaching,[5] gas foaming,[4] electrospinning,[6] and nonwoven techniques.[7] Based on the above methods, SF scaffolds can be fabricated into various forms, including film,[8] hydrogels,[9] nonwoven fabrics,[10] and 3D porous scaffolds.[11] However, SF does not have antimicrobial properties, which often result in wound infection. Thus, how to improve the antimicrobial properties of SF scaffolds is very significant in the use of wound dressing.

Inorganic particles and polymers have been blended with SF to prepare composites,[12] especially for improvement of antimicrobial properties.[13,14] Recent antimicrobial materials focus on cationic polymers, metallic nanoparticles, and antimicrobial peptides. Though metallic nanoparticles, e.g., Ag nanoparticles have a broad spectrum of antimicrobial activity, their cytotoxicity needs to be further studied.[14] Antimicrobial peptides have good biocompatibility, but the high cost limits their wide applications.[15] Thus cationic polymers, especially cationic biomacromolecules, have gained much attention.[13] As one of the natural biomacromolecules, chitosan (CS) has good biocompatibility and intrinsic antimicrobial and hemostasis properties, but with low cost and abundant source. Thus, chitosan and its modified derivatives become favored antimicrobial materials for wound dressings. However, when chitosan was used alone, the poor mechanical properties limit its applications. To improve its mechanical property, many chitosan composites with other polymers have been widely studied.[16]

With the combination of chitosan and SF, CS/SF composites are expected to have good biocompatibility and antimicrobial properties, remarkable permeability and mechanical properties, which are excellent materials for wound dressing. Gobin *et al.* prepared CS/SF-blended scaffolds by freezing-drying method and studied their structure and mechanical properties.[17] She *et al.* found that the CS/SF scaffold was not cytotoxic.[18] CS/SF composite nanofibers have been prepared by electrospinning.[19,20] The composite nanofibers exhibited good biocompatibility for cell proliferation and antimicrobial properties. To improve the water-resistant ability and mechanical properties, aldehyde was used to cross-link electrospun fibers or films.[21] However, the use of CS/SF composite scaffolds in wound dressing was rarely studied *in vivo*. Li *et al.* prepared a sponge wound dressing comprising silk fibroin, *N*-(2-hydroxy)propyl-3-trimethyl ammonium chitosan chloride, and polyvinyl alcohol used for the treatment of chronic wounds in rats and a comparable performance to commercial wound dressing is observed.[22]

Recently, our group prepared SF scaffold with two-photon fluorescence emission properties based on molecular recognition and hydrogen bonding assembly technique,[23] and the fabricated TPF scaffold materials exhibited enhanced two-photon fluorescence efficiency and high-resolution imaging, which were very promising as bioimaging materials. Here, porous SF scaffolds were prepared by a nonwoven technique called *spunlacing technology*, and then CS/SF composite materials were obtained by simply coating a thin layer of CS to SF scaffolds via hydrogen-bonding assembly method. The structure of the composite materials was characterized and the mechanical and antimicrobial properties were measured. Furthermore, the composite scaffolds were used as wound dressings in the rats and the healing mechanism was discussed.

EXPERIMENTAL

Materials

Silk was purchased from silk factory of Qingyang City in China. Chitosan (deacetylase degree >95%) of pharmaceutical grade was purchased from Shanghai Pharmaceutical Corporation. All other reagents including ethanol, acetic acid, hydrogen peroxide, sodium carbonate, and glutaraldehyde were obtained from Shanghai Chemical Reagent Company, which are of analytical grade and used without further purification.

Preparation of Porous SF Scaffolds and SF/CS Composite Scaffolds

Preparation of Porous SF Scaffold. The total process was conducted under ultra-clean biological environment condition. A certain amount of raw silk was put in a 1000 mL beaker, and then 1000 mL deionized water and 5 g Na_2CO_3 were added. The solution was kept at 90°C for 40 min. Then the silk was taken out and washed with deionized water for several times. The sericin was removed and the residue was dried.

The obtained degummed SF fibers were loosen, and cut into small pieces with 3–4 cm length, and then carded into network on the card. The SF network was reinforced by spunlacing with a spunlace rate of 20 Hz at the speed of 2 m/min under 25–55 bar. The resulting SF was cut into small pieces with a diameter of 10 mm and a thickness of *ca* 1.0 mm. The SF scaffold materials were washed with ethanol and deionized water for several times, and dried in a bio-oven at a temperature of 60°C. The mass density of SF scaffold was measured as 100–120 g/m^2.

Preparation of SF/CS Composite Scaffolds. One gram of chitosan was placed in a beaker, and then 50 mL deionized water and 1 mL acetic acid were added. The solution was stirred until chitosan was completely dissolved. The solution was diluted to 1% (w/w) and sprayed onto the SF scaffold (the final mass ratio of CS to SF is 1 : 4). After drying, CS/SF composite scaffolds were obtained and the mass density gives 130–150 g/m^2.

Antimicrobial Performance of SF/CS Composite Scaffolds

The small pieces of composite scaffolds ($d = 10$ mm) were treated by hydrogen peroxide (H_2O_2) and low-temperature plasma sterilization, and then put into the MH-type agar plates containing *Escherichia coli*, *Staphylococcus aureus*, *Pseudomonas aeruginosa*, and *Monilia albicans* at 37°C for 24 h, respectively. The microbial inhibition zones were formed and the diameters were measured. As a controlled experiment, the antimicrobial properties of SF scaffolds without chitosan were also measured.

Cytotoxicity of SF/CS Composite Scaffolds

NCTC clone 929 cells (purchased from Chinese Center for Typical Culture Collection, No.: GDC034) were used here and the cell culture steps were as follows: first, a sterilized scaffold was put into DMEM medium containing 20% serum and soaked overnight. The soaked scaffold was put into 24-well plates, and 0.5 mL cell culture medium with a concentration of 2×10^6/mL was added. The sample was cultured in an incubator (5% CO_2 and 37°C) for 7 days, and the culture medium was changed every 2 days. After that, the scaffold was cleaned with PBS buffer and fixed with 2.5% glutaraldehyde for SEM observation.

The sample preparation for SEM measurements was as follows: First, the above cell sample was rinsed by PBS buffer, fixed with 2.5% glutaraldehyde for 12 h, and then washed with PBS buffer twice. Osmium tetroxide (1%) was used to further fix the sample for 1.5 h, and cleaned with PBS buffer. The dehydration of the sample was first conducted by acetone/isoamyl acetate (1 : 1) for 10 min, and then successively by 50, 70, 80, 90, and 100% ethanol for 15 min. After that, the sample was dried and coated by gold sputtering for SEM images.

Composite Scaffolds as Wound Dressings in the Rat Skin Regeneration

Eight male SD rats were anesthetized by 10% chloral hydrate (100 mg × 0.33 mL). Wounds with diameter ≥1.2 cm were created in the gluteus maximus of rats. Then composite scaffolds were placed on the wounds and closed by medical desensitization tape to observe the healing process. The rats were fed in a single cage after surgery.

Postoperative wounds were regularly observed and the wound surface color, exudates, and granulation tissue bed growth were recorded. The wound size was measured after 1, 3, 6, 14, and 21 days. The nude wound biopsy was conducted after 3, 6, 14, and 21 days. The typical procedure was as follows. The experimental rats were sacrificed by use of air embolism, the desired

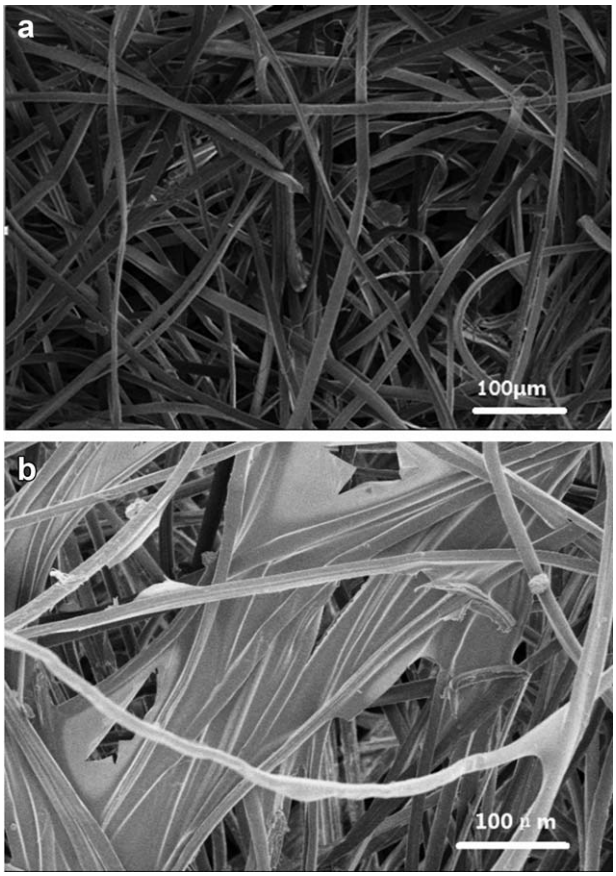

Figure 1. SEM graphs of (a) SF and (b) CS/SF composite scaffold.

area of skin tissue was quickly removed and fixed in 10% formalin. Then the sample was embedded in paraffin, sliced, HE staining, and observed in the light microscope.

Characterization

SEM images were taken from Hitachi S-4800 scanning electron microscope (SEM). Samples were sputter coated with gold before SEM measurements. Fourier transform infrared (FT-IR) spectra were measured using a Nicolex 8700 instrument and recorded in the region 4000–400 cm^{-1} using reflected mode at room temperature. The identification of the crystal phase was carried out using Rigaku D-max-2500 X-ray diffractometer. The mechanical properties of the scaffolds with a dimension of 40 × 20 × 1.0 mm were measured using WDW3020 universal testing machine (Changchun Kexin Equipment Company) at ambient temperature. A cross-head speed of 10 mm/min was used. Each sample was tested for six times, and then the average values and error bars were obtained.

RESULTS AND DISCUSSION

Epidermal damage easily leads to infection, which prevents the healing. SF and CS are both biomacromolecules, and found to promote wound healing. SF has good mechanical properties, but without antimicrobial properties, while CS has good antimicrobial activity, but with poor mechanical properties. Thus their composite materials in the application of wound dressings have been studied. In previous studies, CS/SF nanofibers were prepared by electrospinning[19,20] or CS/SF porous composites were obtained using freezing–drying method from their blends.[17] However, these materials showed poor mechanical properties and is also difficult for large industrial production. Here, porous SF scaffolds made by spunlacing method possessed well mechanical properties besides suitable air and moisture permeability. Simultaneously, the spunlacing method is very simple and propitious to the demand of wholesale industrialization. Thus, the composites can be prepared by simply coating a thin CS layer to SF scaffold via hydrogen-induced assembly technique.

Morphology and Structure of CS/SF Composite Scaffolds

Figure 1 shows the SEM images of SF and CS/SF scaffolds. The average diameter of SF fiber was about 10 μm and its surface was very flat. SF scaffold prepared by spunlacing had a porous structure and the pore size distribution was in the range of 50–200 μm. Owing to the strong hydrogen bonding interactions between CS and SF, CS spread and assembled very uniformly on SF surface and no aggregates were observed [Figure 1(b)]. As a result, the composite scaffold retained the porous structure of the original SF scaffold, but a thin chitosan layer was coated onto the SF scaffold.

Figure 2 shows the FTIR spectra of SF scaffold, chitosan, and CS/SF composite scaffold. The infrared spectra obtained from the chitosan and SF scaffolds displayed all the characteristic peaks reported in literature.[24] In the spectrum obtained from the chitosan, the broad and strong peak around 3400 cm^{-1} was attributed to the intra/inter molecular hydrogen-bonding interaction of —OH and —NH_2 groups, while the carbonyl (CO—NHR) and amine (NH_2) band was located at 1630 cm^{-1}, the amide (C—N) band situated at around 1315 cm^{-1}. Besides, the peaks at 2880 and 2920 cm^{-1} were assigned to the stretching vibration absorption of methylene (—CH_2). The peaks around 1100 cm^{-1} belonged to the vibration of C—O band. SF scaffold exhibited weak peaks at 3286 cm^{-1} arising from the

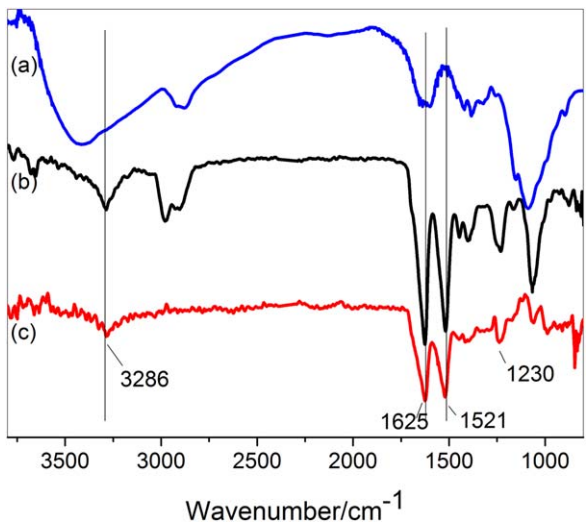

Figure 2. FT-IR patterns of (a) CS, (b) SF/CS composite scaffold, and (c) SF. [Color figure can be viewed in the online issue, which is available at wileyonlinelibrary.com.]

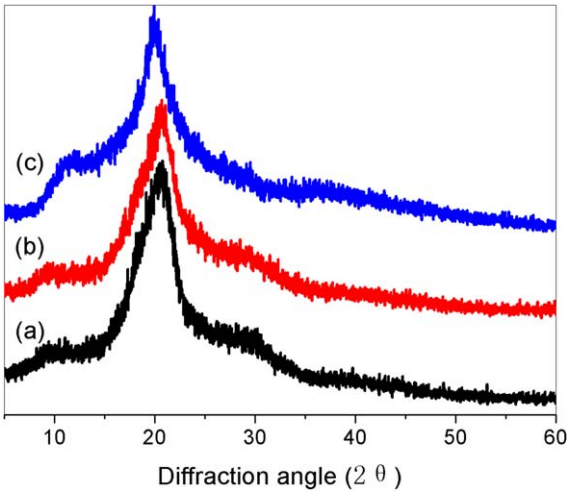

Figure 3. XRD patterns of (a) SF, (b) SF/CS composite scaffold, and (c) CS. [Color figure can be viewed in the online issue, which is available at wileyonlinelibrary.com.]

intra/inter molecular hydrogen bonding interaction between —OH and —NH_2 groups. The characteristic absorption peaks at 1625 cm^{-1} (νC═O, Amide I), 1517 cm^{-1} (νC—N, Amide II), and 1230 cm^{-1} (δN—H, Amide III) all appeared and the absorption bands at 1625 and 1521 cm^{-1} indicated that SF existed as β-sheet in the scaffold.[6] The infrared spectrum of the composite scaffold displayed all the characteristic peaks from chitosan and SF, indicating that chitosan was successfully coated to SF scaffold. The intensity of absorption band at 3286 cm^{-1} was much stronger than that of SF scaffold, suggesting that the molecular interactions were enhanced after chitosan coating. Because there are many —OH and —NH_2 groups in chitosan and SF molecules, the increased molecular interactions resulted mainly from hydrogen-bonding interactions between chitosan and SF. Based on the strong driving force of hydrogen-bonding interactions, a uniform assembly of chitosan on the SF scaffold was achieved, in agreement with SEM images in Figure 1(b). The strong absorption bands at 1625 and 1521 cm^{-1} in the composite scaffold demonstrated that SF still existed as β-sheet conformation.

Figure 3 shows the X-ray diffraction patterns of chitosan, SF, and CS/SF composite scaffolds. Chitosan had characteristic diffraction peaks at 11.0° and 19.9°,[25] while the characteristic diffraction peaks of β-sheet appeared at 9.60° and 20.4° in SF scaffold.[26] The diffraction patterns of CS/SF composite scaffold was almost the same as that of SF scaffold, suggesting that SF kept β-sheet conformation in the composite materials, consistent with the FTIR data. However, the peak at 20.4° became broad and its intensity decreased, indicating that hydrogen-bonding interactions between chitosan and SF molecules weakened the intra/intermolecular interactions in SF, resulting in a decrease of crystallinity.

Mechanical Properties of CS/SF Composite Scaffolds

Figure 4 shows the mechanical properties of SF and CS/SF composite scaffolds. Compared with that of SF scaffold, the tensile strength of the composite scaffolds was greatly improved from 5 to 13 MPa, accompanying with a decrease of strain at break from 22.5 to 8.3%, because of the strong hydrogen-bonding interactions between chitosan and SF, consistent with FTIR and XRD data. As a result, the hardness of the composite scaffolds increased and the flexibility reduced.

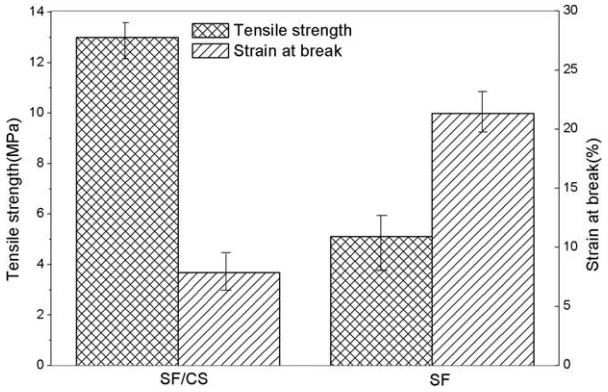

Figure 4. Mechanical properties of SF and SF/CS composite scaffolds.

Antimicrobial Properties of CS/SF Composite Scaffolds

Figure 5 shows the results of antimicrobial tests with SF and CS/SF composite scaffolds. No inhibitory ring formed for SF scaffold after 24 h treatment, while the composite scaffolds had good antimicrobial properties in either of four tested microbials owing to the intrinsic antimicrobial properties of chitosan.[21,27] The antimicrobial ability of CS/SF composite scaffolds depended on the type of microbial. The diameters of inhibitory rings for *E. coli*, *S. aureus*, *P. aeruginosa*, and *M. albicans* were 31, 14, 22, and 11 mm, respectively, showing that the composite scaffolds had the strongest antimicrobial properties in *S. aureus* and the weakest in *M. albicans*. In all, the above experiments demonstrated that the composite scaffolds had a broad spectrum of antimicrobial properties.

Cytotoxicity of SF/CS Composite Scaffolds

To study the cytotoxicity of CS/SF composite, SEM was used to observe the cell attachment and proliferation on the scaffolds. As shown in Figure 6, after 7 days of culture, cells had a good proliferation along the scaffold and pseudopodia formed. This suggested that CS/SF composite scaffolds were not cytotoxic and had good biocompatibility, which provided a huge probability in the following rat skin regeneration experiments.

Composite Scaffolds as Wound Dressings in the Rat Skin Regeneration

Figure 7 shows the postoperative wounds in rats with the healing time. On the day of surgery, bilateral showed no bleeding tendency, which suggested the composite scaffolds had a better hemostasis. Three days later, all wounds belonged to the normal physiological changes, and no infection was observed. After 6 days, the wound diameter was reduced to 0.9 cm, and wound scab formed. After 14 days, crusting shrink became faster and the wounds diameter was only 0.3 cm. After 21 days, there were no obvious wounds left, the wounds were completely healed.

Figure 8 shows the pathological photos at different periods from surgery. After 3 days, bleeding occurred in the skeletal muscle mass, fiber cell degeneration, and necrosis accompanying

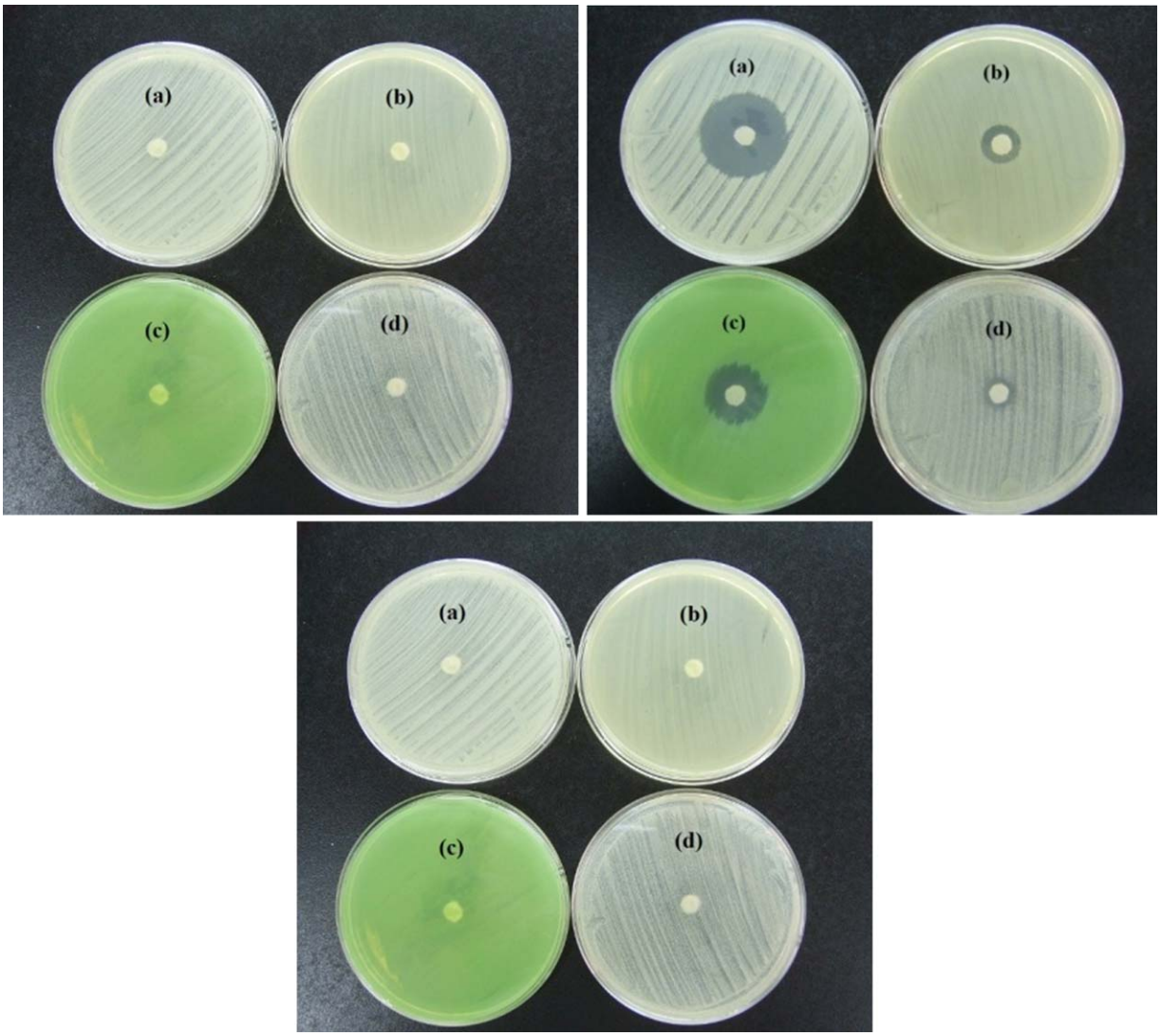

Figure 5. (1) Photos of CS/SF composite scaffolds before microbial culture, (2) photos of CS/SF composite scaffolds after 24 h microbial culture, (3) photos of SF scaffolds after 24 h microbial culture. (a–d) Four kinds of microbials are *Escherichia coli*, *Staphylococcus aureus*, *Pseudomonas aeruginosa*, and *Monilia albicans*, respectively. [Color figure can be viewed in the online issue, which is available at wileyonlinelibrary.com.]

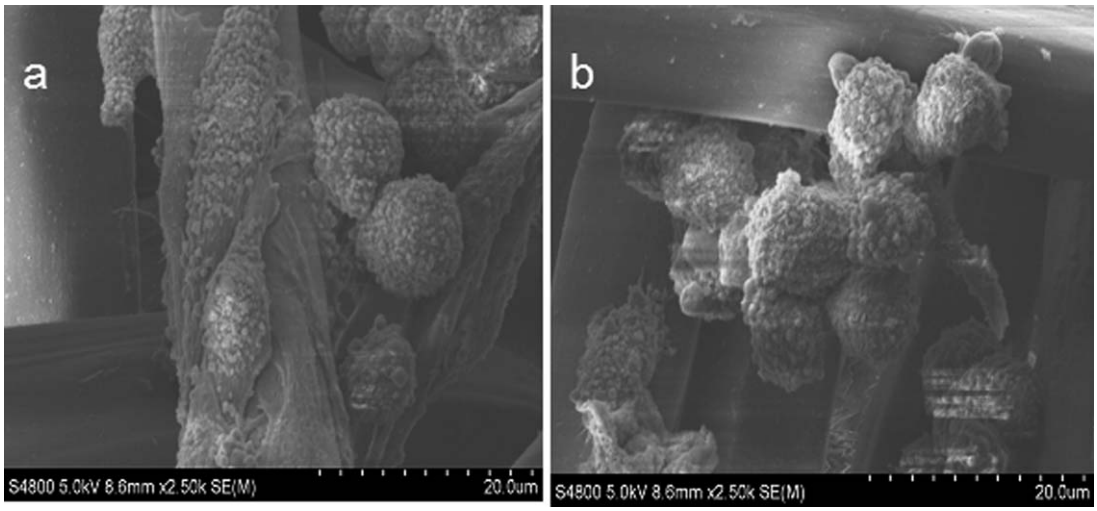

Figure 6. SEM images of L929 cells proliferation on the surface of SF/CS scaffolds at different culture time. (a) 0 day; (b) 7 days.

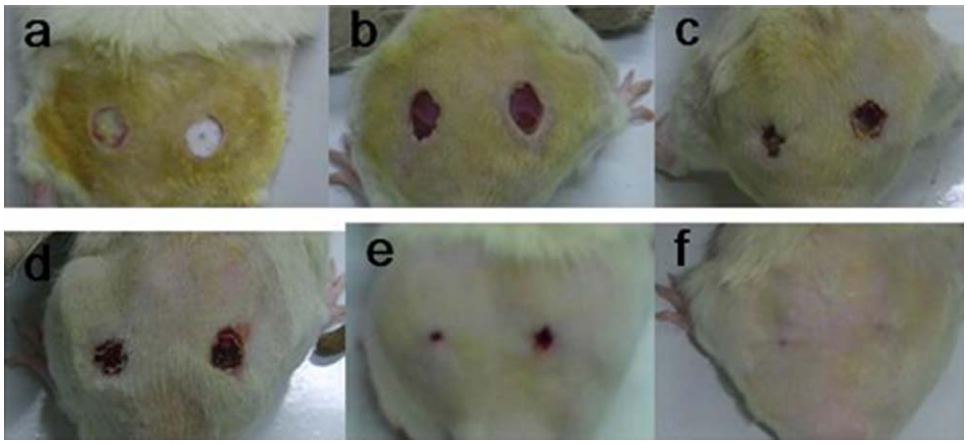

Figure 7. Macroscopic observation of rat skin wound healing after different days since surgery. (a) 0 day; (b) 1 day; (c) 3 days; (d) 6 days; (e) 14 days; (f) 21 days. [Color figure can be viewed in the online issue, which is available at wileyonlinelibrary.com.]

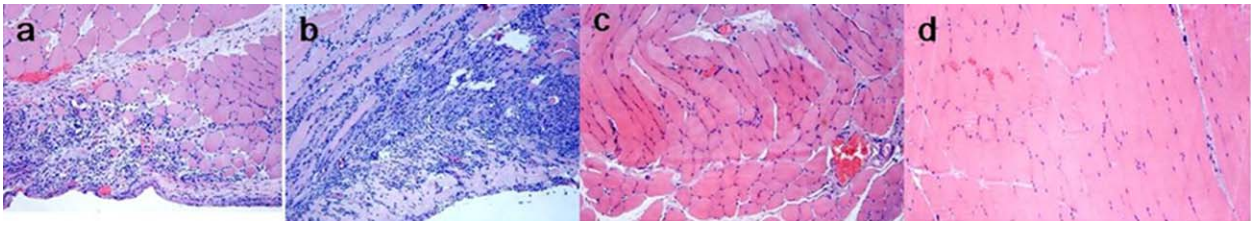

Figure 8. Hematoxylin–eosin staining of regenerative skin after different days since surgery. (a) 3 days; (b) 6 days; (c) 14 days; and (d) 21 days. Magnification: 50×. [Color figure can be viewed in the online issue, which is available at wileyonlinelibrary.com.]

with inflammatory cell infiltration were observed. After 6 days, skeletal muscle fiber necrosis, inflammatory cell infiltration, and fibroblast proliferation appeared. After 14 days and even 21 days, there were no pathological changes in skeletal muscle fiber cells. These results suggested that CS/SF composite scaffolds had no teratogenic effects in rats and could be used as medical dressings for skin regeneration. The mechanism of composite scaffolds in wound healing was that first, the coated chitosan formed viscous gels on the wound surface with exudates and blood, so that the wounds could maintain a certain temperature, humidity, and a part of exudate nutrients, providing a favorable environment for wound healing. Second, the good mechanical properties and biocompatibility of the composite scaffolds promoted cell absorption and proliferation, and the porous structure was beneficial for the nutrition and oxygen support. Furthermore, the intrinsic strong antimicrobial properties of chitosan prevented the infection and favored a quick healing.

CONCLUSIONS

Porous CS/SF composite scaffolds were successfully prepared by coating a thin chitosan layer onto SF scaffolds via hydrogen-bonding interactions, which were confirmed by FTIR and XRD. The composite scaffolds exhibited well mechanical properties, strong antimicrobial properties, and good biocompatibility, thus they can be used as wound dressings. *In vivo* experiments of rats indicated that CS/SF composite scaffolds could promote wound healing and skin regeneration in rats without any teratogenic effect and inflection, which had good potential in tissue engineering.

ACKNOWLEDGMENTS

This research was financially supported by the National Natural Science Fund of China (Grant Nos. 51372004, 21271040 and 21171034), Ph.D. Program Foundation of Ministry of Education of China (No.20070255012), Shanghai Municipal Natural Science Foundation for Youths (No. 12ZR144100), and "Chen Guang" project (No. 12CG37) supported by Shanghai Municipal Education Commission and Shanghai Education Development Foundation.

REFERENCES

1. Ovington, L. G. *Clin. Dermato.* **2007**, *25*, 33.
2. Boateng, J. S.; Matthews, K. H.; Stevens, H. N. E.; Eccleston, G. M. *J. Pharm. Sci.* **2008**, *97*, 2892.
3. Sasaki, M.; Kato, Y.; Yamada, H.; Terada, S. *Biotechnol. Appl. Biochem.* **2005**, *42*, 183.
4. Nazarov, R.; Jin, H. J.; Kaplan, D. L. *Biomacromolecules* **2004**, *5*, 718.
5. Seth, A.; Chung, Y. G.; Gil, E. S.; Tu, D.; Franck, D.; Vizio, D. D.; Adam, R. M.; Kaplan, D. L.; Estrada, C. R.; Mauneya, J. R. *Biomaterials* **2013**, *34*, 4758.
6. Khan, M. M. R.; Tsukada, M.; Zhang, X. H.; Morikawa, H. *J. Mater. Sci.* **2013**, *48*, 3731.

7. Dal Pra, I.; Freddi, G.; Minic, J.; Chiarini, A.; Armato, U. *Biomaterials* **2005**, *26*, 1987.
8. Gil, E. S.; Panilaitis, B.; Bellas, E.; Kaplan, D. L. *Adv. Healthc. Mater.* **2013**, *2*, 206.
9. Zhong, T. Y.; Xie, Z. G.; Deng, C. M.; Chen, M.; Gao, Y. F.; Zuo, B. Q. *J. Appl. Polym. Sci.* **2013**, *127*, 2019.
10. Chutipakdeevong, J.; Ruktanonchai, U. R.; Supaphol, P. *J. Appl. Polym. Sci.* **2013**, *130*, 3634.
11. Asakura, T.; Saotome, T.; Aytemiz, D.; Shimokawatoko, H.; Yagi, T.; Fukayama, T.; Ozai, Y.; Tanaka, R. *RSC Adv.* **2014**, *4*, 4427.
12. Siritientong, T.; Ratanavaraporn, J.; Srichana, T.; Aramwit, P. *Biomed. Res. Int.* **2013**, *13*, 904314.
13. De Simone, S.; Gallo, A. L.; Paladini, F.; Sannino, A.; Pollini, M. *J. Mater. Sci.* **2014**, *25*, 2205.
14. Calamak, S.; Erdogdu, C.; Ozalp, M.; Ulubayram, K. *Mater Sci Eng. C.* **2014**, *43*, 11.
15. Gibney, K. A.; Sovadinova, I.; Lopez, A. I.; Urban, M.; Ridgway, Z.; Caputo, G. A.; Kuroda, K. *Macromol. Biosci.* **2012**, *12*, 1279.
16. Jayakumar, R.; Prabaharan, M.; Kumar, P. T. S.; Nair, S. V.; Tamura, H. *Biotechnol. Adv.* **2011**, *29*, 322.
17. Gobin, A. S.; Froude, V. E.; Mathur, A. B. *J. Biomed. Mater. Res. A* **2005**, *74A*, 465.
18. She, Z. D.; Jin, C. R.; Huang, Z.; Zhang, B. F.; Feng, Q. L.; Xu, Y. X. *J. Mater. Sci.* **2008**, *19*, 3545.
19. Zhao, R.; Li, X.; Sun, B. L.; Zhang, Y.; Zhang, D. W.; Tang, Z. H.; Chen, X. S.; Wang, C. *Int. J. Biol. Macromol.* **2014**, *68*, 92.
20. Cai, Z. X.; Mo, X. M.; Zhang, K. H.; Fan, L. P.; Yin, A. L.; He, C. L.; Wang, H. S. *Int. J. Mol. Sci.* **2010**, *11*, 3529.
21. Gu, Z. P.; Xie, H. X.; Huang, C. C.; Li, L.; Yu, X. X. *Int. J. Biol. Macromol.* **2013**, *58*, 121.
22. Li, X. M.; Li, B. H.; Ma, J.; Wang, X. Y.; Zhang, S. M. *J. Bioact. Compat. Pol.* **2014**, *29*, 398.
23. Lin, N. B.; Liu, X. Y.; Diao, Y. Y.; Xu, H. Y.; Chen, C. Y.; Ouyang, X. H.; Yang, H. Z.; Ji, W. *Adv. Funct. Mater.* **2012**, *22*, 361.
24. Haider, S.; Park, S. Y. *J. Membr. Sci.* **2009**, *328*, 90.
25. Wang, S. F.; Shen, L.; Tong, Y. J.; Chen, L.; Phang, I. Y.; Lim, P. Q.; Liu, T. X. *Polym. Degrad. Stab.* **2005**, *90*, 123.
26. Kim, S. H.; Nam, Y. S.; Lee, T. S.; Park, W. H. *Polym. J.* **2003**, *35*, 185.
27. Sun, X. X.; Wang, Z.; Kadouh, H.; Zhou, K. Q. *LWT-Food Sci. Technol.* **2014**, *57*, 83.